Des-A-lupane in an East African lake sedimentary record as a new proxy for the stable carbon isotopic composition of C$_3$ plants

L.G.J. van Bree [a,b,*], W.I.C. Rijpstra [a], N.A. Al-Dhabi [c], D. Verschuren [d], J.S. Sinninghe Damsté [a,b], J.W. de Leeuw [a,b]

[a] NIOZ Royal Netherlands Institute for Sea Research, Department of Marine Microbiology and Biogeochemistry, Utrecht University, PO Box 59, 1790 AB Den Burg, The Netherlands
[b] Utrecht University, Faculty of Geosciences, Department of Earth Sciences, PO Box 80.115, 3508 TC Utrecht, The Netherlands
[c] Department of Botany and Microbiology, Addiriyah Chair for Environmental Studies, College of Science, King Saud University, P.O. Box 2455, Riyadh 11451, Saudi Arabia
[d] Ghent University, Limnology Unit, K.L. Ledeganckstraat 35, B-9000 Gent, Belgium

A B S T R A C T

We studied the high-resolution and well-dated 25,000 year sedimentary record of Lake Challa, a deep tropical crater lake in equatorial East Africa, to explore new proxies for paleoenvironmental and paleohydrological change. Sedimentary biomarker analysis revealed the presence of *des*-A-triterpenoids with oleanane, ursane and lupane carbon skeletons, microbial degradation products of angiosperm plant triterpenoids. Their increased influx from 16,000 years ago corresponds with previously documented changes in the terrestrial vegetation of the Lake Challa basin during postglacial warming, in particular the relative increase in C$_3$/C$_4$ plant ratio inferred from the stable carbon isotopic signature (δ^{13}C) of sedimentary *n*-alkanes derived from plant leaf waxes. In contrast to this *n*-alkane δ^{13}C signature, the δ^{13}C of *des*-A-lupane maintains a constant value of $-27.4 \pm 1.1\permil$ across the glacial–interglacial transition. Since *des*-A-lupane is derived from C$_3$ plants, its δ^{13}C signature is here proposed to represent a novel and independent proxy for the time-variable carbon isotopic composition of local terrestrial C$_3$ plants, which can improve estimates of the C$_3$/C$_4$ plant ratio based on two-end member mixing models of *n*-alkane δ^{13}C values.

© 2016 Elsevier Ltd. All rights reserved.

1. Introduction

Non-hopanoid pentacyclic triterpenoids preserved in lake and marine sediments are relatively well studied biomarkers, and used in organic geochemistry as a proxy for the input of terrestrial angiosperm plants (e.g., Rullkötter et al., 1982; Freeman et al., 1994; Sabel et al., 2005). These wax components are synthesized almost exclusively by higher plants as a defense mechanism against insects, pathogens and herbivores (Langenheim, 1994). Pentacyclic triterpenoids with, for example, lupane, oleanane and ursane skeletons, are widely accepted as general biomarkers for angiosperms, yet most of these triterpenoids are not species-specific (e.g., Ohmoto et al., 1970; ten Haven and Rullkötter, 1988; Regnery et al., 2013). *Des*-A-triterpenoids, in turn, are diagenetic products of triterpenoid A-ring degradation (Trendel et al., 1989), a process probably mediated by microorganisms under anoxic conditions (Lohmann et al., 1990).

Plant wax lipids, such as *n*-alkanes, can be used as indicators of the composition of local vegetation, as their compound-specific stable carbon isotopic value (δ^{13}C) depends on the dominant biochemical pathway used by plants for photosynthesis. Higher plants usually fix CO$_2$ by either the C$_3$ (Calvin-Benson) or C$_4$ (Hatch-Slack) cycle. In C$_4$ photosynthesis, atmospheric CO$_2$ entering the plant stomata is pre-concentrated, resulting in less carbon isotopic depletion. In tropical Africa, lowland vegetation consists mostly of C$_4$ grasses and C$_3$ trees and shrubs, and (seasonal) moisture availability is the dominant control on the distribution and abundance of these C$_4$ grasses across the modern-day landscape. On glacial–interglacial time scales, variation in atmospheric pCO$_2$ exerted an important control on the composition of savanna vegetation of East Africa (Sinninghe Damsté et al., 2011). When pCO$_2$ varies little, as within the Holocene, the distribution of C$_3$ and C$_4$ vegetation can be used as a measure of past water availability (Castañeda et al., 2007).

During an earlier high-resolution stratigraphic study of *n*-alk-1-enes in the continuous and well-dated 25,000 year (25 kyr) sedimentary record of Lake Challa, a deep crater lake in equatorial East Africa (van Bree et al., 2014), we also encountered a wide range of

des-A-triterpenoids. In this paper, we report our findings regarding the origin and potential paleoenvironmental application of the pentacyclic triterpenoid degradation products derived from higher plants. A study of *des*-A-arborenes/fernenes also present in Lake Challa sediments, but of microbial origin, will be published separately.

2. Material and methods

2.1. Study area

Lake Challa (3°19′S, 37°42′E) is a relatively unproductive, tropical freshwater lake, situated ~880 m above sea level on the lower south-eastern slope of Mt. Kilimanjaro (Fig. 1). Shared by Kenya and Tanzania, it has a surface area of 4.5 km², a steep-sided crater catchment of ~3.4 km² and a maximum depth of ~90 m. Rainfall seasonality is mainly determined by the semi-annual passing of the Inter-Tropical Convergence Zone (ITCZ), resulting in moderate 'long rains' (March–May) and more intense 'short rains' (October–December) separated by a long dry season during Southern Hemisphere winter (June–September). Since the local balance between precipitation and evaporation is negative by three to one, the lake's water budget must be maintained by substantial groundwater inflow, derived from rainfall on the forested mid-elevation slopes of Mt. Kilimanjaro. Also temporary creek discharge breaching the crater's northwestern rim can occur during very heavy rains (Buckles et al., 2014). Daily wind-driven mixing of the water column is limited to the uppermost 15–20 m year round. Seasonal deeper mixing (June–September) extends to 40–60 m, implying a permanently stratified lower water column. Given limited density stratification, the possibility of complete mixing cannot be excluded but its recurrence frequency is likely decadal or longer, rather than inter-annual (Wolff et al., 2011, 2014). Wind-blown (aeolian) particles, supplemented by soil and litter input from the steep-sided inner slopes of the crater, contribute allochthonous organic matter to Lake Challa sediments. The vegetation outside the crater and on top of the rim is a woodland-savannah with shrubs, trees and C₄ grasses, while inside the crater rim a more varied vegetation occurs, including CAM plants in a dry succulent forest occupying the middle slopes, and a fringe of evergreen forest around the lake shore (Hemp, 2006; Sinninghe Damsté et al., 2011).

2.2. Study material

A 21.65 m composite core of mostly finely laminated organic muds was retrieved from the center of Lake Challa (Fig. 1) during coring activities in 2003 and 2005 (Verschuren et al., 2009). This yielded, after excision of five turbidites, a 20.82 m long master sequence covering the last 25 kyr of continuous offshore lacustrine sedimentation. The age-depth model is based on a smoothed spline through INTCAL04-calibrated AMS ¹⁴C ages of 164 bulk organic carbon samples (Blaauw et al., 2011). For this study, a total of 148 sediment samples with 4 cm thickness was extracted and processed for biomarker analysis, generally at ~200 year intervals, with a higher resolution of ~50 year intervals in the youngest 3.2 kyr. In addition, we analyzed the compound-specific δ¹³C values of selected biomarkers in 52 sediment samples distributed throughout the sequence.

In order to trace the origin of the biomarkers found in Lake Challa sediments, we further analyzed soil and litter samples from around the lake, suspended particulate matter (SPM) and settling particles collected by a sediment trap (Sinninghe Damsté et al., 2009; Buckles et al., 2014). This sediment trap was deployed at 35 m water depth in a usually suboxic part of
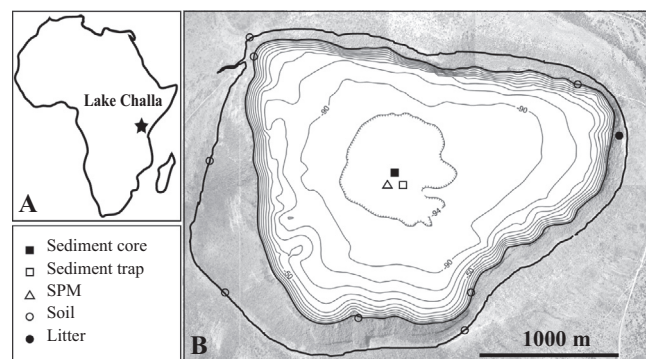

Fig. 1. (A) Location of Lake Challa (3°19′S, 37°42′E) in equatorial East Africa; (B) Lake Challa and its crater basin with bathymetry at 10 m intervals and sampling locations of the suspended particulate matter (SPM) profile (△), the sediment trap (□) and the 25,000 year sediment record (■), as well as catchment soils (○) and litter (●). The outer bold line indicates the crater rim, which defines the lake's catchment area. Modified after Moernaut et al. (2010) and van Bree et al. (2014).

the water column, and samples were retrieved at ca. 4 week intervals between November 2006 and December 2007 (Sinninghe Damsté et al., 2009). The SPM sampling was conducted on 10–11 September 2006 along a vertical profile in the center of the lake, every 5 m between 0 and 30 m, and every 10 m between 30 and 90 m water depth. The water samples (4–9 L) were filtered through GF/F filters and stored frozen until processed. Eight soil samples were collected from within the catchment area of Lake Challa in 2005 (Sinninghe Damsté et al., 2009; Fig. 1). Sampling of litter in September 2012 included three near-shore samples representing leaf and fruit remains from forest trees and shrubs, and two samples from just below the crater rim consisting of leaf and twig remains and small non-diagnostic organic debris. These samples were also stored frozen until analysis.

2.3. Lipid extraction

The freeze-dried and powdered sediment samples were extracted with a Dionex™ Accelerated Solvent Extractor (ASE), using a dichloromethane (DCM)/methanol (9:1, v:v) mixture at high temperature (100 °C) and pressure (7.6 × 10⁶ Pa) (Sinninghe Damsté et al., 2011). The total extracts were separated over an activated Al₂O₃ column into an apolar and a polar fraction with hexane/DCM (9:1, v:v) and DCM/MeOH (1:1, v:v), respectively. Accumulation rates of apolar compounds (in mg/m²y) were calculated based on their concentration, the wet weight and water content of the sediment samples, and the sediment's age-depth profile. For analysis of stable carbon isotopic composition, a subset of the apolar fractions were separated into a saturated and an unsaturated hydrocarbon fraction using a small Ag⁺-impregnated silica column with hexane and ethyl acetate as eluents, respectively.

SPM and sediment trap samples were extracted previously (Sinninghe Damsté et al., 2009). Fluxes of apolar compounds (in mg/m²y) in the sediment trap samples were calculated using the concentration of each of these components relative to total particle flux.

Litter and soil samples were extracted ultrasonically with DCM/MeOH (2:1, v:v), after cutting the larger leaf, stem or fruit remains into small pieces. The extracts were evaporated to dryness, methylated with diazomethane in diethyl ether and separated over an activated Al₂O₃ column into apolar, ketone and polar fractions, using hexane/DCM (9:1, v:v), hexane/DCM (1:1, v:v) and DCM/MeOH (1:1, v:v) as eluents, respectively.

Table 1
List of *des*-A-triterpenoids in the Lake Challa sediment record with retention times, mass spectral data and (tentative) identifications.

Peak number	Retention time (GC–MS)	Most significant ions (in order of decreasing abundance)	M⁺	Formula	Tentative identification	References
1	18.16	109, 313, 189, 328 [M⁺], 205, 204, 218, 161	328	$C_{24}H_{40}$	*Des*-A-olean-13(18)-ene	A B C D E
2	18.30	203, 218, 313, 189, 328 [M⁺], 231, 243	328	$C_{24}H_{40}$	*Des*-A-olean-12-ene	A B D
3	18.52	313, 177, 189, 121, 175, 328 [M⁺], 218	328	$C_{24}H_{40}$	*Des*-A-urs-13(18)-ene	A B D
4	19.01	218, 203, 313, 189, 133, 328 [M⁺], 231	328	$(C_{24}H_{40})$	Mixture, *i.a. des*-A-ursenes	
5	19.60	123, 149, 163, 191, 287, 206, 330 [M⁺], 315	330	$C_{24}H_{42}$	*Des*-A-lupane	A C D E F G

References: A: Corbet (1980); B: Logan and Eglinton (1994); C: Trendel et al. (1989); D: Jacob et al. (2007); E: Huang et al. (2008); F: Schmitter et al. (1981); G: Boreham et al. (1994).

2.4. Lipid identification and quantification

The apolar fractions of sediments, SPM, sediment trap, soil and litter extracts were analyzed by gas chromatography (GC) and GC–mass spectrometry (GC–MS), after addition of a known amount of internal standard. A few polar fractions of sediment and SPM samples were methylated, silylated and screened for functionalized triterpenoids.

GC was performed using a Hewlett-Packard (HP6890) instrument equipped with an on-column injector and a flame ionization detector (FID). A fused silica capillary column (25 m × 0.32 mm) coated with CP Sil-5 CB (film thickness 0.12 μm) was used with helium as carrier gas. The samples were injected at 70 °C and the oven temperature was programmed to rise at 20 °C/min to 130 °C, and then at 4 °C/min to 320 °C, at which it was held for 20 min.

GC–MS was performed on a Finnigan Trace DSQ mass spectrometer operated at 70 eV with a mass range of *m/z* 40–800 and a cycle time of 1.7 s. The gas chromatograph was equipped with a fused silica capillary column as described above. The carrier gas was helium and the same oven temperature program as for GC was used. Identification of the *des*-A-triterpenoids and other triterpenoid hydrocarbons is based on relative retention times, published mass spectra (including the NIST98 spectral library), and interpretation of observed fragmentation patterns. Quantification of compounds was performed by peak area integration of appropriate peaks (including that of the internal standard) in the FID chromatograms.

2.5. Compound-specific carbon isotope analyses

We subjected 52 saturated hydrocarbon fractions to compound-specific $\delta^{13}C$ analysis using an Agilent 6800 GC coupled to a ThermoFisher Delta V isotope-ratio monitoring mass spectrometer. The isotope values were measured with reference to a calibrated external reference gas, and performance of the instrument was monitored daily by injections of a mixture of C_{20} and C_{24} perdeuterated *n*-alkanes with known isotopic composition. The $\delta^{13}C$ values are reported in standard delta notation against the Vienna Pee Dee Belemnite (VPDB). All samples were run at least in duplicate, allowing estimation of the standard deviation of these measurements. $\delta^{13}C$ values of the *n*-alkanes in these same samples have been published previously (Sinninghe Damsté et al., 2011).

3. Results

3.1. The sedimentary record of des-A-triterpenoids in Lake Challa

Our analysis of the apolar fractions of 148 biomarker extracts from Lake Challa sediments covering the last 25 kyr showed the presence of *n*-alkanes, *n*-alk-1-enes, phytadienes, aromatic triterpenoids, hopenes, and a suite of *des*-A-triterpenoid hydrocarbons with lupane, oleanane, ursane, and fernane or arborane skeletons. The stratigraphic distribution, origin and palaeoenvironmental significance of the *n*-alkanes and *n*-alk-1-enes have been discussed by Sinninghe Damsté et al. (2011) and van Bree et al. (2014), respectively.

We detected 11 distinct *des*-A-triterpenoid hydrocarbon compounds on the basis of their relative retention times, published mass spectra, and interpretation of mass spectrometric fragmentation patterns. The mass spectra of ten *des*-A-triterpenes and one *des*-A-triterpane exhibit molecular ions at *m/z* 324, 326, 328 or 330. In this paper we focus on the distribution, origin and potential paleoenvironmental application of the five *des*-A-triterpenoids with lupane, oleanane and ursane skeletons (Fig. 2A). The identification and geochemical significance of the other, arborane- or fernane-derived *des*-A-triterpenoids will be discussed elsewhere. In addition to these *des*-A-triterpenoids with arborane or fernane skeletons, several other, non-identified *des*-A-triterpenoids co-eluted, occurred infrequently or were present in low relative abundance and are not further discussed.

Compound **1** (M⁺· at *m/z* 328; Fig. 2B) was identified as *des*-A-olean-13(18)-ene (Corbet, 1980; Logan and Eglinton, 1994; Jacob et al., 2007; Huang et al., 2008), and compound **2** (M⁺· at *m/z* 328; Fig. 2B) was tentatively assigned to *des*-A-olean-12-ene (Corbet, 1980; Logan and Eglinton, 1994; Jacob et al., 2007). *Des*-A-triterpenoid **3** (M⁺· at *m/z* 328; Fig. 2B) was identified as *des*-A-urs-13(18)-ene (Corbet, 1980; Logan and Eglinton, 1994; Jacob et al., 2007). Compound **4** (M⁺· at *m/z* 328; Fig. 2B) represents a mixture of *des*-A-ursenes, which could not be further identified. *Des*-A-triterpenoid **5** exhibiting an M⁺· at *m/z* 330 (Fig. 2B) was identified as *des*-A-lupane (Corbet, 1980; Schmitter et al., 1981; Trendel et al., 1989; Boreham et al., 1994; Jacob et al., 2007; Huang et al., 2008).

The accumulation rates (in mg/m²y) of these *des*-A-triterpenoid hydrocarbons in the sedimentary record vary considerably over time (Fig. 3). The stratigraphic distributions of *des*-A-triterpenoids with lupane (**5**), ursane (**3**) and oleanane (**1** + **2**) skeletons are all similar and significantly inter-correlated: *des*-A-lupane with *des*-A-oleanenes ($R^2 = 0.53$), *des*-A-oleanenes with *des*-A-ursene ($R^2 = 0.62$) and *des*-A-lupane with *des*-A-ursene ($R^2 = 0.81$). Throughout the record, *des*-A-lupane is more abundant than *des*-A-ursene, whereas the concentration of *des*-A-oleanenes is lowest (Fig. 3). They all exhibit low accumulation rates from 25,000 to 15,000 years ago (the glacial and early post-glacial period) and much higher (on average 5–11 times) accumulation rates in last 12,000 years (the Holocene).

The $\delta^{13}C$ values of *des*-A-lupane (Fig. 4) vary between −25.1‰ and −29.4‰ (−27.4‰ ± 1.1‰ on average) with no significant trend over time ($R^2 = 0.042$; $n = 38$; $p = 0.22$). Determinations of $\delta^{13}C$ values of other *des*-A-triterpenoids of the oleanane and ursane type in the unsaturated hydrocarbon fraction were unsuccessful due to co-elution or low abundances.

3.2. Triterpenoids and des-A-triterpenoids in soil and litter surrounding the lake

No *des*-A-triterpenoids were identified in the hydrocarbon fraction of extracts from soils and litter. Functionalized triterpenoids in
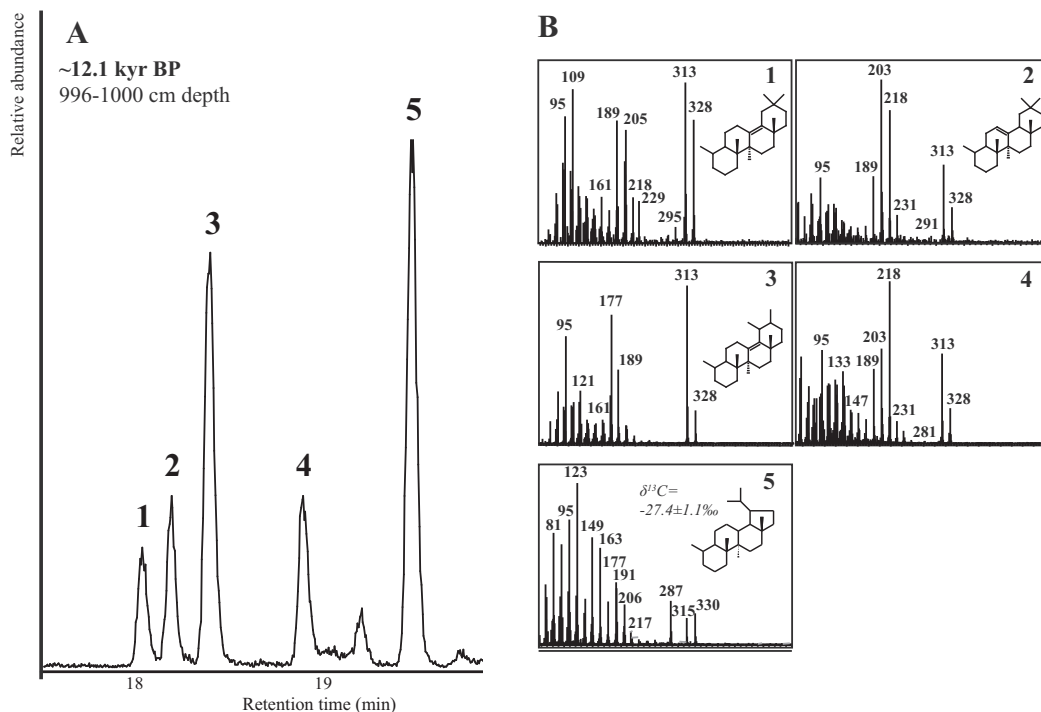
Fig. 2. Higher plant derived *des*-A-triterpenoids in the Lake Challa sediments. Panel (A) shows a partial summed mass chromatogram (*m/z* 163 + 177 + 189 + 203 + 218 + 309) of the distribution of *des*-A-triterpenoids in the apolar fraction of the lipid biomarker extract from 996–1000 cm core depth, deposited ~12.1 kyr BP. Panel (B) shows the electron-impact mass spectra of *des*-A-triterpenoids in the Lake Challa sediment record: *des*-A-olean-13(18)-ene (compound **1**); *des*-A-olean-12-ene (**2**); *des*-A-urs-13(18)-ene (**3**); mixture of *des*-A-ursenes (**4**); *des*-A-lupane (**5**). Additional information on these compounds is presented in Table 1.

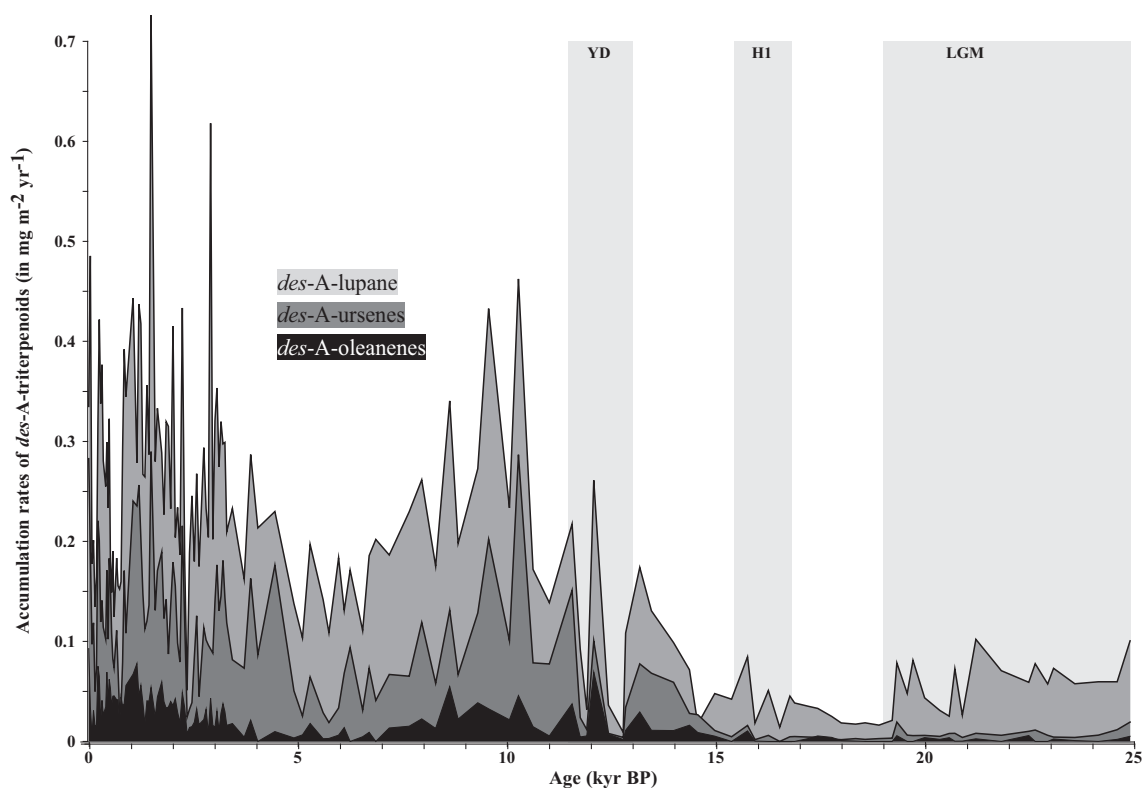**Fig. 3.** Variation through time in the accumulation rates (in mg/m²y, not cumulative) of the *des*-A-triterpenoid compounds for *des*-A-lupane, *des*-A-ursenes and *des*-A-oleanenes in Lake Challa sediments. Shaded areas represent the LGM (26.5–19 kyr BP), Heinrich event H1 (16.8–15.4 kyr BP) and YD (13–11.5 kyr BP).

soils along the crater rim (Fig. 1) were identified as urs-12-en-3β-ol (α-amyrin), olean-12-en-3β-ol (β-amyrin), olean-13(18)-en-3β-ol, ursa-9(11),12-dien-3-one, taraxerone, lup-20(29)-en-3-one,

lup-20(29)-en-3β-ol acetate and friedelan-3-one and, tentatively, methyl-ursa-2,12-dien-28-oate. Also three pentacyclic triterpene methyl ethers (PTMEs) with oleanane and taraxerane skeletons
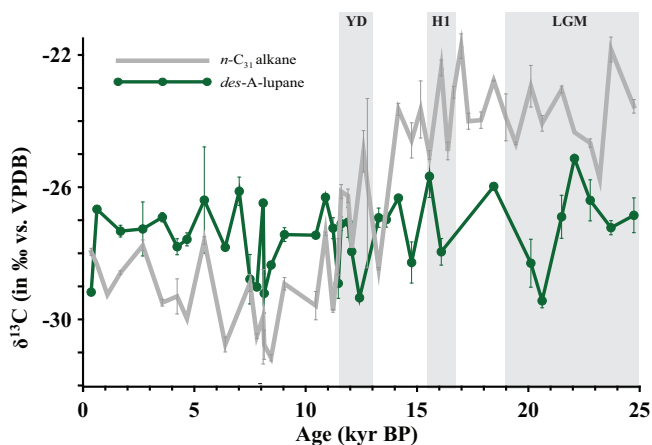
Fig. 4. Variation through time in the stable carbon isotopic composition ($\delta^{13}C$, in ‰ vs VPDB) of n-C_{31} alkanes (Sinninghe Damsté et al., 2011) and *des*-A-lupane (this study).

were detected: 3β-methoxy-olean-12-ene (iso-sawamilletin; β-amyrin ME), 3β-methoxy-olean-18-ene ME (miliacin; germanicol ME) and 3β-methoxy-taraxer-14-ene (sawamilletin, crusgallin or taraxerol ME). Litter samples contained the oleanane-type triterpenoids β-amyrenone, olean-18-en-3β-one (germanicone), olean-18-en-3β-ol (germanicol) and β-amyrin acetate. The functionalized ursane-type triterpenoids present were α-amyrinone and α-amyrin acetate. One litter sample contained a lupeol acetate.

3.3. Des-A-triterpenoids in sedimenting particles and suspended particulate matter

In the extracts of sedimenting particles, only low concentrations of *des*-A-urs-13(18)-ene and *des*-A-lupane were detected, together with traces of functionalized triterpenoids such as α-amyrin. Hydrocarbon concentrations in the SPM extracts were too low for identification of specific triterpenoid compounds.

4. Discussion

The strong correlation between accumulation rates of *des*-A-oleanenes, *des*-A-ursene and *des*-A-lupane (Fig. 3) suggest a common origin for these *des*-A-triterpenoids. Higher plant material originates predominantly from washed-in debris of local terrestrial vegetation from within the crater catchment, because of the absence of riverine input, the limited amount of leaf waxes deposited from the air, and the near-absence of submerged or emergent aquatic macrophytes due to the steep crater walls both above and below the lake surface (Sinninghe Damsté et al., 2011). While various *des*-A-triterpenoid hydrocarbons are present both in the sediment record and to some extent in settling particles, these compounds are lacking in the collected litter and soil. *Des*-A-triterpenoids are thought to result from microbial degradation of functionalized triterpenoids, under anoxic or reducing conditions (e.g., Lohmann et al., 1990; Jacob et al., 2007; Huang et al., 2008); their presence in the sediment trap material indicates that microbial degradation is not restricted to the anoxic lower water column in Lake Challa. One other mechanism for *des*-A-triterpenoids to enter the system, namely the washing-in of microbial degradation products from (anoxic) soils, is unlikely in Lake Challa, as the studied litter and soils did not contain *des*-A-triterpenoids.

The principal degradation processes affecting pentacyclic triterpenoids have been described by various authors (e.g., Trendel et al., 1989; Hauke et al., 1992a, 1992b; Jacob et al., 2007), although not

all transformation routes are completely established. Early diagenetic degradation of C-3 oxygenated triterpenoids involves either A to D-ring aromatization or the loss of the A-ring, followed by progressive aromatization from ring B to D (Trendel et al., 1989; Lohmann et al., 1990). The dominant transformation pathway of non-hopanoid triterpenoids in Lake Challa sediments is loss of the A-ring. This loss can be initiated by the formation of A-seco-intermediates, a process that can already occur within the vegetation by photochemical or photomimetic influences (Corbet, 1980; Baas, 1985), but in Lake Challa sediments such intermediates were not identified.

4.1. Des-A-oleanenes and des-A-ursenes

Oleanane- and ursane-type triterpenoids are generally considered to be biomarkers of terrestrial higher plants, specifically angiosperms (e.g., Diefendorf et al., 2012). Smetanina et al. (2001) identified miliacin (3β-methoxy-olean-18-ene) in a marine fungus, which would imply that oleanoid-type triterpenoids are not exclusively produced by terrestrial higher plants. However, a new study on this fungal species did not yield any miliacin (Bossard et al., 2013). We therefore consider all oleanane- and ursane-type triterpenoids as angiosperm biomarkers.

Functionalized triterpenoids with ursane and oleanane skeletons occur in the local vegetation, soils and litter of Lake Challa, often as α- or β-amyrin. The accumulation of their *des*-A-counterparts in the sediments increased markedly from 15 kyr BP onwards (Fig. 3). A comparatively low accumulation of higher plant *des*-A-triterpenes occurred during the C_4 plant dominated glacial and early late-glacial periods (Sinninghe Damsté et al., 2011; Fig. 4), suggesting that the C_4 grasses which dominated the vegetation inside the crater at that time did not produce (much of these) triterpenoids. The increase in higher plant *des*-A-triterpenoid accumulation after 15 kyr BP (Fig. 3) broadly coincides with the shift toward a mixed C_3/C_4 vegetation as inferred from $\delta^{13}C$ signature of n-C_{31} alkanes (Fig. 4; Sinninghe Damsté et al., 2011) and palynological data (van Geel et al., 2011), following the post-glacial intensification of the region's monsoon rainfall (Verschuren et al., 2009).

Concentrations of *des*-A-oleanenes in Lake Challa sediments are relatively low compared to the other *des*-A-triterpenoids, especially considering the predominance of oleanane-type functionalized triterpenoids in the investigated soils and litter. Future studies on the hydrocarbons in local Lake Challa vegetation might shed light on this apparent discrepancy. Possibly, aromatization of some triterpenoid types is favored over the loss of the A-ring, although the low and infrequent occurrence of aromatic triterpenoids in the sedimentary record does not seem to fit this scenario.

4.2. Des-A-lupane: a tracer of C_3 plant vegetation composition

The only saturated *des*-A-triterpenoid present in Lake Challa sediments is *des*-A-lupane, as has also been reported from other late-Quaternary lake sediment records (e.g., Jacob et al., 2007; Huang et al., 2008). This saturation may be a result of its specific precursors such as lupeol, lupanol or lupanone, or because *des*-A-lupane is more resistant to diagenesis compared to other saturated *des*-A-triterpenoids (Jacob et al., 2007; Huang et al., 2008).

Des-A-lupane records have been interpreted in different ways. Huang et al. (2008), who studied the Dajiuhu peat deposit in China, used *des*-A-lupane as a proxy for the depositional environment at the time of burial, linking sections of the biomarker record with more *des*-A-lupane to episodes of limited degradation (i.e. better preservation). This mechanism is less likely to apply to Lake Challa, because of its relatively constant sedimentation rate and continuously anoxic bottom-water conditions. In a study on the Brazilian

Lake Caçó, *des*-A-lupane was thought to be derived from a belt of spike-rush (*Eleocharis* sp.), an emergent aquatic macrophyte (Jacob et al., 2007). As already mentioned, aquatic macrophytes are not a likely source of organic matter input in Lake Challa, as the shoreline of Lake Challa is rocky and near-vertical (Fig. 1), which largely prevents aquatic macrophyte growth. Even substantial lake-level lowering, which occurred during the early late-glacial period (Moernaut et al., 2010), is not expected to have created more favorable conditions for development of aquatic macrophytes (Sinninghe Damsté et al., 2011). Given the absence of functionalized triterpenoids in the sedimentary record of Lake Challa, we consider the sedimentary *des*-A-lupane record (Fig. 3) to reflect the input of its precursors in the lake, with a constant transformation of these precursors into *des*-A-lupane, and minor or no degradation of *des*-A-lupane over the last 25 kyr.

Most non-hopanoid triterpenoids are not species-specific, and the lupane-type triterpenoids are no exception. Although these compounds occur in both C_3 and C_4 plants (e.g., Misra et al., 1988; Macías-Rubalcava et al., 2007; Saleem, 2009; Singariya et al., 2012, 2014), the specific $\delta^{13}C$ value of *des*-A-lupane ($-27.4‰$ on average, SD = $\pm1.1‰$, $n = 38$; Fig. 4) clearly indicates a C_3 plant origin (cf. Castañeda et al., 2009; Diefendorf et al., 2012). Regnery et al. (2013) reported a comparable $\delta^{13}C$ signature (ranging from $-28‰$ to $-30.6‰$) of *des*-A-lupane in lake sediments from the Holsteinian interglacial (cf. Marine Isotope Stage 11c) at Dethlingen in Germany, also similar to *des*-A-lupane isotope values in Tertiary brown coal from China ($-28.1 \pm 0.6‰$; Schoell et al., 1994). Some genera of the Betulaceae (birch family) biosynthesize *des*-A-lupane precursors and, therefore, this C_3 plant family is regularly designated as an important biological source of *des*-A-lupane (Regnery et al., 2013; Schnell et al., 2014). However, Betulaceae do not naturally occur in tropical Africa and no Betulaceae vegetation or pollen are found in Lake Challa (Sinninghe Damsté et al., 2011; van Geel et al., 2011), so in this setting, *des*-A-lupane must originate from other C_3 plant species.

In line with Regnery et al. (2013), and in contrast to Jacob et al. (2007), Huang et al. (2008) and Diefendorf et al. (2012), the concentration of *des*-A-lupane in Lake Challa sediments correlates well with oleanane- and ursane-type *des*-A-triterpenoids. We propose that this dichotomy can be explained by one or more different sources of *des*-A-lupane in these latter studies.

An interesting feature of the *des*-A-lupane $\delta^{13}C$ record is the apparent lack of trend over longer timescales (Fig. 4). This record does show some variability over time, but, unexpectedly, no trend, even though large changes in pCO_2 (and its carbon isotopic composition), rainfall and vegetation occur over the glacial–interglacial transition. Recently it was shown that carbon isotope discrimination in C_3 land plants is independent of natural variations in pCO_2 (e.g., Kohn, 2016). Furthermore, the $\delta^{13}C$ value of CO_2 varies by only ~1‰ (between $-7‰$ and $-6‰$) over the LGM and Holocene, a variability that is hard to differentiate within the analytical error of compound-specific $\delta^{13}C$ analysis. Lastly, the modest variability in the *des*-A-lupane $\delta^{13}C$ record in Lake Challa that does occur shows no clear connection to the regional vegetation changes and the alternation of wetter and drier periods documented from other proxies. This absence of a clear trend in $\delta^{13}C$ values of *des*-A-lupane was also noted by Regnery et al. (2013) in their interglacial record from Dethlingen paleolake.

Recent studies have indicated the need for more direct proxies of C_3 and C_4 higher plants (Diefendorf et al., 2010; Castañeda and Schouten, 2011), and our findings may be an important step in this development. Firstly, the concentration of *des*-A-triterpenoids with ursane/oleanane/lupane skeletons in the Lake Challa record is high when C_3 plants (trees and shrubs) are common in local/regional vegetation (Sinninghe Damsté et al., 2011; van Geel et al., 2011). Therefore, we might be able to use these compounds as an absolute

measure of C_3 plant abundance, instead of the usual estimate of C_3 or C_4 percentage based on variation in *n*-alkane $\delta^{13}C$ values. Secondly, we introduce a new way of estimating the average $\delta^{13}C$ value of C_3 vegetation at any point in time, which can be important for carbon cycle studies, as $\delta^{13}C$ records of C_3 plants could be used by modelers to assess the possible pCO_2-effect of plant $\delta^{13}C$ (Kohn, 2016). Thirdly, we can use this C_3 plant-specific $\delta^{13}C$ record for improving estimates of the C_3/C_4 ratio in past vegetation. Recently, the relative contribution of C_3 and C_4 plants in terrestrial vegetation has been modeled using the $\delta^{13}C$ value of long-chain *n*-alkanes (e.g., Castañeda et al., 2007; Sinninghe Damsté et al., 2011; Berke et al., 2012). In the Holocene section of our Lake Challa record, *des*-A-lupane $\delta^{13}C$ values are on average less depleted ($-27.6‰$) than those of the *n*-C_{31} alkane ($-29.1‰$; Sinninghe Damsté et al., 2011); the situation is reversed during the glacial period, where average *des*-A-lupane $\delta^{13}C$ values ($-27.2‰$) are more depleted than those of *n*-C_{31} alkanes ($-24.3‰$; Sinninghe Damsté et al., 2011). During the Holocene period, C_3 plants are estimated to contribute ca. 50% of the *n*-C_{31} alkanes (Sinninghe Damsté et al., 2011). This value was calculated using a simple binary box model, in which a 50/50 mixture of C_3- and C_4-derived alkanes (with mean values of respectively $-35.2‰$ and $-21.7‰$ in modern plants; Castañeda et al., 2009) yields an average $\delta^{13}C$ value of $-28.5‰$. During the glacial period, vegetation in the Lake Challa region was dominated by C_4 grasses; the mixed C_3/C_4 composition developed only from 16.5 kyr BP onwards (Sinninghe Damsté et al., 2011), when a riparian forest of C_3 trees and shrubs started growing inside the crater (van Geel et al., 2011). This local growth of C_3 vegetation is also clearly evident in the record of *des*-A-triterpenoid hydrocarbons with lupane, ursane and oleanane skeletons (Fig. 3).

The carbon isotopic fractionation between acetyl CoA-based compounds (e.g., *n*-alkanes) and the isoprene-based isoprenoids essentially depends on the biosynthetic pathways by which they are produced (e.g., MVA for isoprenoids in angiosperms). In their study of North American C_3 plants, Diefendorf et al. (2012) showed that this biosynthetic offset between terpenoids and *n*-alkanes is ~4–6‰. Correspondingly, also in sedimentary records, the ^{13}C of terpenoids is typically reported to be enriched by 5–6‰ compared to *n*-alkanes. We do not expect this biosynthetic offset between triterpenoids and *n*-alkanes to be different in East African vegetation. Temperate C_3 plants may have significantly lower 'overall' lipid fractionation values compared to tropical species (Diefendorf et al., 2011), but this will influence the *n*-alkanes and the terpenoids in the same way. Hence, we can use the $\delta^{13}C$ of *des*-A-lupane as a temporal (i.e. time-specific) C_3 endmember in modeling the C_3/C_4 ratio of local vegetation. To this end we subtracted an average terpenoid enrichment of 5.5‰ from the individual *des*-A-lupane $\delta^{13}C$ values to estimate the $\delta^{13}C$ values of *n*-C_{31} alkanes derived from local C_3 plants at each time interval. We use the average offset as recorded in sediments (Diefendorf et al., 2012) for this down-core correction exercise, as sediments contain more integrated, averaged signals compared to fresh plant material. Introduction of these corrected *n*-C_{31} alkane $\delta^{13}C$ values in the binary box model for C_3/C_4 ratio calculation, using a constant *n*-C_{31} alkane $\delta^{13}C$ value of $-21.7‰$ derived from C_4 plants (cf. Castañeda et al., 2009), results in an estimated increase in the relative proportion of C_3 plants by 0% and 19% (Fig. 5) as compared to values obtained by Sinninghe Damsté et al. (2011). Our %C_3 estimates are different from the previous estimates (*t*-test; $p < 0.0001$, $n = 35$), and the difference remains significant throughout the terpenoid to *n*-alkane offset range of 4–6‰ (i.e. the range that exists in modern plants; Diefendorf et al., 2012). From this exercise we conclude that especially in the Holocene part of the Lake Challa record, when local vegetation had a mixed C_3/C_4 composition, a reconstruction using fixed C_3 plant $\delta^{13}C$ values underes-
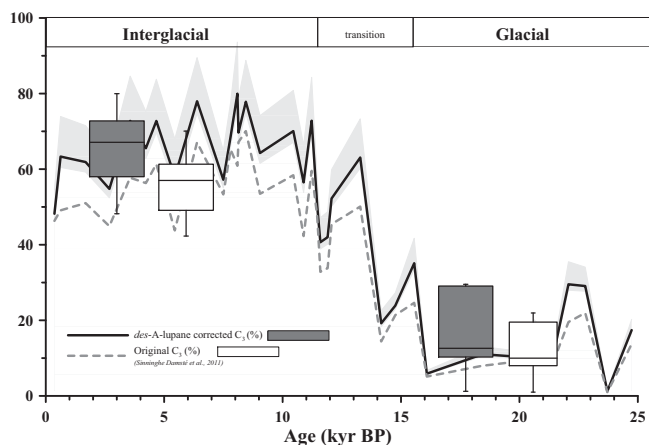
Fig. 5. Percentage of C$_3$ vegetation, based on n-C$_{31}$ alkane δ^{13}C values (data from Sinninghe Damsté et al., 2011), calculated in two different ways: first (solid line) using *des*-A-lupane as the local and temporally variable C$_3$ plant endmember and an average terpenoid fractionation of 5.5‰ relative to the *n*-alkanes, and second (dashed line) based on fixed δ^{13}C values for the C$_3$ plant (-35.2‰) and C$_4$ plant (-21.7‰) endmembers taken from the literature (Sinninghe Damsté et al., 2011). The range of C$_3$ estimates when the modern terpenoid fractionation range of 4–6‰ is taken into account is plotted as a gray band. Boxplots show the differences between the original and *des*-A-lupane (gray, left-hand side) corrected C$_3$ estimate in the glacial and early late-glacial (25–16 kyr BP) and in the interglacial period (Holocene, 12.3–0 kyr BP) (thus excluding the glacial–interglacial transition), with median, first and third quartiles, and whiskers depicting the minimum/maximum values.

timates the fraction of C$_3$ vegetation, while there is less discrepancy during the glacial and early late-glacial periods when C$_4$ plants (here mostly grasses) were dominant. This result is especially valuable for carbon-cycle modeling studies, where correct assessment of climate–vegetation feedbacks strongly depends on correct estimates of past C$_3$/C$_4$ (and hence biome) distribution.

Our method for time-specific correction of the fraction of C$_3$ plants in local vegetation has the potential to enhance the accuracy of C$_3$/C$_4$ vegetation reconstructions in all situations where the local C$_3$ plant signal is as strong as during the Holocene around Lake Challa (Fig. 5). Using sample-specific *des*-A-triterpenoid δ^{13}C values for estimating this local C$_3$ vegetation component is convenient, as for example *des*-A-lupane is present in the saturated aliphatic lipid fraction, just like the *n*-alkanes, and can therefore be measured in the same analysis.

5. Conclusions

We investigated the possibility of using the degradation products of terrestrial higher plant pentacyclic triterpenoids as a proxy for local vegetation reconstructions. The accumulation of *des*-A-triterpenoids with oleanane/ursane/lupane skeletons serves as a proxy record for the local abundance of C$_3$ vegetation. The δ^{13}C signature of *des*-A-lupane can be used as a proxy for the stable carbon isotopic composition of local C$_3$ plants if, as in our study site of Lake Challa, *des*-A-lupane is exclusively of C$_3$ plant origin. Therefore, it can be applied as a temporally variable C$_3$ plant end member representing the local C$_3$ vegetation component in reconstructions of the C$_3$/C$_4$ ratio through time.

Acknowledgements

Associate Editor—**Marcus Elvert**

References

Baas, W.J., 1985. Naturally occurring *seco*-ring-A-triterpenoids and their possible biological significance. Phytochemistry 24, 1875–1889.

Berke, M.A., Johnson, T.C., Werne, J.P., Grice, K., Schouten, S., Sinninghe Damsté, J.S., 2012. Molecular records of climate variability and vegetation response since the Late Pleistocene in the Lake Victoria basin, East Africa. Quaternary Science Reviews 55, 59–74.

Blaauw, M., van Geel, B., Kristen, I., Plessen, B., Lyaruu, A., Engstrom, D.R., van der Plicht, J., Verschuren, D., 2011. High-resolution ^{14}C dating of a 25,000-year lake-sediment record from equatorial East Africa. Quaternary Science Reviews 30, 3043–3059.

Boreham, C.J., Summons, R.E., Roksandic, Z., Dowling, L.M., Hutton, A.C., 1994. Chemical, molecular and isotopic differentiation of organic facies in the Tertiary lacustrine Duaringa oil shale deposit, Queensland, Australia. Organic Geochemistry 21, 685–712.

Bossard, N., Jacob, J., Le Milbeau, C., Sauze, J., Terwilliger, V., Poissonnier, B., Vergès, E., 2013. Distribution of miliacin (olean-18-en-3β-ol methyl ether) and related compounds in broomcorn millet (*Panicum miliaceum*) and other reputed sources: implications for the use of sedimentary miliacin as a tracer of millet. Organic Geochemistry 63, 48–55.

Buckles, L.K., Weijers, J.W.H., Verschuren, D., Sinninghe Damsté, J.S., 2014. Sources of core and intact branched tetraether membrane lipids in the lacustrine environment: anatomy of Lake Challa and its catchment, equatorial East Africa. Geochimica et Cosmochimica Acta 140, 106–126.

Castañeda, I.S., Werne, J.P., Johnson, T.C., 2007. Wet and arid phases in the southeast African tropics since the Last Glacial Maximum. Geology 35, 823–826.

Castañeda, I.S., Mulitza, S., Schefuß, E., Lopes dos Santos, R.A., Sinninghe Damsté, J.S., Schouten, S., 2009. Wet phases in the Sahara/Sahel region and human migration patterns in North Africa. Proceedings of the National academy of Sciences of the United States of America 106, 20159–20163.

Castañeda, I.S., Schouten, S., 2011. A review of molecular organic proxies for examining modern and ancient lacustrine environments. Quaternary Science Reviews 30, 2851–2891.

Corbet, B., 1980. Origine et transformation des triterpènes dans les sédiments récents Ph.D. Thesis. Université Louis Pasteur, Strasbourg, France, p. 106.

Diefendorf, A.F., Mueller, K.E., Wing, S.L., Koch, P.L., Freeman, K.H., 2010. Global patterns in leaf ^{13}C discrimination and implications for studies of past and future climate. Proceedings of the National academy of Sciences of the United States of America 103, 5738–5743.

Diefendorf, A.F., Freeman, K.H., Wing, S.L., Graham, H.V., 2011. Production of *n*-alkyl lipids in living plants and implications for the geological past. Geochimica et Cosmochimica Acta 75, 7472–7485.

Diefendorf, A.F., Freeman, K.H., Wing, S.L., 2012. Distribution and carbon isotope patterns of diterpenoids and triterpenoids in modern temperate C$_3$ trees and their geochemical significance. Geochimica et Cosmochimica Acta 85, 342–356.

Freeman, K.H., Boreham, C.J., Summons, R.E., Hayes, J.M., 1994. The effect of aromatization on the isotopic compositions of hydrocarbons during early diagenesis. Organic Geochemistry 21, 1037–1049.

Hauke, V., Graff, R., Wehrung, P., Trendel, J.M., Albrecht, P., 1992a. Novel triterpene-derived hydrocarbons of arborane/fernane series in sediments. Part I. Tetrahedron 48, 3915–3924.

Hauke, V., Graff, R., Wehrung, P., Trendel, J.M., Albrecht, P., Riva, A., Hopfgartner, G., Gülaçar, F.O., Buchs, A., Eakin, P.A., 1992b. Novel triterpene-derived hydrocarbons of arborane/fernane series in sediments. Part II. Geochimica et Cosmochimica Acta 56, 3595–3602.

Hemp, A., 2006. Continuum or zonation? Altitudinal gradients in the forest vegetation of Mt. Kilimanjaro. Plant Ecology 184, 27–42.

Huang, X., Xie, S., Zhang, C.L., Jiao, D., Huang, J., Yu, J., Jin, F., Gu, Y., 2008. Distribution of aliphatic *des*-A-triterpenoids in the Dajiuhu peat deposit, southern China. Organic Geochemistry 39, 1765–1771.

Jacob, J., Disnar, J.R., Boussafir, M., Albuquerque, A.L.S., Sifeddine, A., Turcq, B., 2007. Contrasted distributions of triterpene derivatives in the sediments of Lake Caçó reflect paleoenvironmental changes during the last 20,000 yrs in NE Brazil. Organic Geochemistry 38, 180–197.

Kohn, M.J., 2016. Carbon isotope discrimination in C$_3$ land plants is independent of natural variations in pCO$_2$. Geochemical Perspective Letters 2, 35–43.

Langenheim, J.H., 1994. Higher plant terpenoids: a phytocentric overview of their ecological roles. Journal of Chemical Ecology 20, 1223–1280.

Logan, G.A., Eglinton, G., 1994. Biogeochemistry of the Miocene lacustrine deposit, at Clarkia, northern Idaho, U.S.A. Organic Geochemistry 21, 857–870.

Lohmann, F., Trendel, J.M., Hetru, C., Albrecht, P., 1990. C-29 tritiated β-amyrin: chemical synthesis aiming at the study of aromatization processes in sediments. Journal of Labelled Compounds & Radiopharmaceuticals 28, 377–386.

Macías-Rubalcava, M.L., Hernández-Bautista, B.E., Jiménez-Estrada, M., Cruz-Ortega, R., Anaya, A.L., 2007. Pentacyclic triterpenes with selective bioactivity from *Sebastiania adenophora* leaves, Euphorbiaceae. Journal of Chemical Ecology 33, 147–156.

Misra, S., Choudhury, A., Chattopadhyay, S., Ghosh, A., 1988. Lipid composition of *Porteresia coarctata* from two different mangrove habitats in India. Phytochemistry 27, 361–364.

Moernaut, J., Verschuren, D., Charlet, F., Kristen, I., Fagot, M., De Batist, M., 2010. The seismic-stratigraphic record of lake-level fluctuations in Lake Challa: hydrological stability and change in equatorial East Africa over the last 140 kyr. Earth and Planetary Science Letters 290, 214–223.

Ohmoto, T., Ikuse, M., Natori, S., 1970. Triterpenoids of the Gramineae. Phytochemistry 9, 2137–2148.

Regnery, J., Püttmann, W., Koutsodendris, A., Mulch, A., Pross, J., 2013. Comparison of the paleoclimatic significance of higher land plant biomarker concentrations and pollen data: a case study of lake sediments from the Holsteinian interglacial. Organic Geochemistry 61, 73–84.

Rullkötter, J., Leythaeuser, D., Wendisch, D., 1982. Novel 23,28-bisnorlupanes in Tertiary sediments. Widespread occurrence of nuclear demethylated triterpanes. Geochimica et Cosmochimica Acta 46, 2501–2509.

Sabel, M., Bechtel, A., Püttmann, W., Hoernes, S., 2005. Palaeoenvironment of the Eocene Eckfeld Maar lake (Germany): implications from geochemical analysis of the oil shale sequence. Organic Geochemistry 36, 873–891.

Saleem, M., 2009. Lupeol. A novel anti-inflammatory and anti-cancer dietary triterpene. Cancer Letters 285, 109–115.

Schmitter, J.M., Arpino, P.J., Guiochon, G., 1981. Isolation of degraded pentacyclic triterpenoid acids in a Nigerian crude oil and their identification as tetracyclic carboxylic acids resulting from ring A cleavage. Geochimica et Cosmochimica Acta 45, 1951–1955.

Schnell, G., Schaeffer, P., Tardivon, H., Motsch, E., Connan, J., Ertlen, D., Schwartz, D., Schneider, N., Adam, P., 2014. Contrasting diagenetic pathways of higher plant triterpenoids in buried wood as a function of tree species. Organic Geochemistry 66, 107–124.

Schoell, M., Simoneit, B.R.T., Wang, T.G., 1994. Organic geochemistry and coal petrology of Tertiary brown coal in the Zhoujing mine, Baise Basin, South China – 4. Biomarker sources inferred from stable carbon isotope compositions of individual compounds. Organic Geochemistry 21, 713–719.

Singariya, P., Kumar, P., Mourya, K.K., 2012. Isolation of some new steroids and evaluation of bio-activity of *Cenchrus ciliaris*. International Journal of Research in Pharmaceutical Sciences 3, 678–684.

Singariya, P., Kumar, P., Mourya, K.K., 2014. Isolation of new steroids of Kala Dhaman grass (*Cenchrus setigerus*) and evaluation of their bioactivity. Brazilian Archives of Biology and Technology 57, 62–69.

Sinninghe Damsté, J.S., Ossebaar, J., Abbas, B., Schouten, S., Verschuren, D., 2009. Fluxes and distribution of tetraether lipids in an equatorial African lake: constraints on the application of the TEX_{86} palaeothermometer and BIT index in lacustrine settings. Geochimica et Cosmochimica Acta 73, 4232–4249.

Sinninghe Damsté, J.S., Verschuren, D., Ossebaar, J., Blokker, J., van Houten, R., van der Meer, M.T.J., Plessen, B., Schouten, S., 2011. A 25,000-year record of climate-induced changes in lowland vegetation of eastern equatorial Africa revealed by the stable carbon-isotopic composition of fossil plant leaf waxes. Earth and Planetary Science Letters 302, 236–246.

Smetanina, O.F., Kuznetzova, T.A., Denisenko, V.A., Pivkin, M.V., Khudyakova, Y.V., Gerasimenko, A.V., Popov, D.Y., Il'in, S.G., Elyakov, G.B., 2001. 3β-Methoxyolean-18-ene (miliacin) from the marine fungus *Chaetomium olivaceum*. Russian Chemical Bulletin 50, 2463–2465.

ten Haven, H.L., Rullkötter, J., 1988. The diagenetic fate of taraxer-14-ene and oleanene isomers. Geochimica et Cosmochimica Acta 10, 2543–2548.

Trendel, J.M., Lohmann, F., Kintzinger, J.P., Albrecht, P., Chiarone, A., Riche, C., Cesario, M., Guilhem, J., Pascard, C., 1989. Identification of *des*-A-triterpenoid hydrocarbons occurring in surface sediments. Tetrahedron 6, 4457–4470.

van Bree, L.G.J., Rijpstra, W.I.C., Cocquyt, C., Al-Dhabi, N.A., Verschuren, D., Sinninghe Damsté, J.S., de Leeuw, J.W., 2014. Origin and palaeo-environmental significance of C_{25} and C_{27} *n*-alk-1-enes in a 25,000-year lake-sedimentary record from equatorial East Africa. Geochimica et Cosmochimica Acta 145, 89–102.

van Geel, B., Gelorini, V., Lyaruu, A., Aptroot, A., Rucina, S., Marchant, R., Sinninghe Damsté, J.S., Verschuren, D., 2011. Diversity and ecology of tropical African fungal spores from a 25,000-year palaeoenvironmental record in southeastern Kenya. Review of Palaeobotany and Palynology 164, 174–190.

Verschuren, D., Sinninghe Damsté, J.S., Moernaut, J., Kristen, I., Blaauw, M., Fagot, M., Haug, G.H., 2009. Half-precessional dynamics of monsoon rainfall near the East African Equator. Nature 462, 637–641.

Wolff, C., Haug, G.H., Timmermann, A., Sinninghe Damsté, J.S., Brauer, A., Sigman, D.M., Cane, M.A., Verschuren, D., 2011. Reduced interannual rainfall variability in East Africa during the Last Ice Age. Science 333, 743–747.

Wolff, C., Kristen-Jenny, I., Schettler, G., Plessen, B., Meyer, H., Dulski, P., Naumann, R., Brauer, A., Verschuren, D., Haug, G.H., 2014. Modern seasonality in Lake Challa (Kenya/Tanzania) and its sedimentary documentation in recent lake sediments. Limnology and Oceanography 59, 1621–1636.